RESEARCH ARTICLE

Laser-selective melting and forming technology for CNTs/Al composites

Shengkai Li*

Department of Intelligent Manufacturing, Huainan Union University, Huainan, Anhui, China

Received: June 21, 2023; **accepted:** August 18, 2023.

With the development and widespread application of high tech, complex industrial production increases the requirements for the performance and structure of metal materials. In order to improve the performance of metal materials and reduce industrial production costs, a laser selective melting forming method for carbon nanotubes (CNTs)/ aluminum (Al) composite materials was proposed. The composite material powder was prepared by wet mixing followed by ball milling method. CNTs and N-methylpyrrolidone (NMP) were mixed and dispersed using an ultrasonic cleaning machine for 40 minutes to reduce the compactness of CNTs clusters. Then, a finite element model for laser selective melting forming of CNTs/Al composite materials was constructed, and its application effect was tested and analyzed. The results showed that the density of aluminum based composite materials could reach up to 95%. The wear coefficient remained around 0.3, which was reduced by 0.35 compared to aluminum alloy materials. The highest strength and conductivity were 410 MPa and 68%, respectively, which were 240 MPa and 50% International Annealed Copper Standard (IACS) higher than that of aluminum alloy materials. The coefficient of thermal expansion remained at stable levels above 7×10^{-6} /K. Therefore, the addition of CNTs in laser selective melting forming of aluminum matrix composites had optimized the mechanical properties of aluminum matrix composites, improved conductivity, thermal stability, and wear resistance, and broadened the application range of aluminum matrix composites.

Keywords: carbon nanotubes; laser-selective melting; aluminum matrix composites; microstructure.

***Corresponding author:** Shengkai Li, Department of Intelligent Manufacturing, Huainan Union University, Huainan 232001, Anhui, China. Email: lishengkai2023@outlook.com.

Introduction

Carbon nanotubes (CNTs) are a one-dimensional nanomaterial with stable structure. Although they have strong tensile strength and hardness, they have good flexibility and light weight. CNTs can not only conduct electricity but also transfer heat, and have performance advantages in mechanics, electronics, and chemistry. Combined with other materials, CNTs can improve the elasticity, toughness, and fatigue resistance of composite materials, and has broad application prospects [1, 2]. CNTs have a perfect tubular structure and are widely used in fields such as smart furniture and wearable devices. Many researchers have conducted research on it. Xue, *et al*. investigated the electromagnetic wave absorption ability of carbon-based composites derived from metal organic frameworks [3]. Based on pyrolysis, a caterpillar-like layered structure of CNTs had been prepared. The results showed that the composite material could have strong absorption effects at different frequencies, while reducing conduction losses, providing a new approach for the manufacturing of electromagnetic wave absorption materials. Bairagi and Ali focused on the impact of CNTs on the piezoelectric performance of electrospun

nanogenerators and analyzed the corresponding generator performance by controlling the concentration of CNTs [4]. The results showed that, when the concentration of CNTs in the composite material was 0.1 wt%, the performance of the nanogenerator was significantly improved. At the same time, the conductivity of electrospun fibers was strengthened, verifying the effectiveness of this method in wearable products. Wang, *et al*. prepared a hybrid shape memory matrix by combining trans-1,4-polyisoprene (TPI) with high density polyethylene (HDPE) to improve the limitations of 4-polyisoprene shape memory and incorporated it into CNTs to form a memory matrix [5]. The experimental results demonstrated that CNTs acted as nucleating agents, facilitating the formation of TPI and HDPE crystal structures, while enhancing the thermal and mechanical properties of the composite material. Khan, *et al*. innovatively studied the fluidity of CNTs Porous medium between turntables based on entropy optimization, constructed the entropy generative model of nanoparticles, and analyzed the flow parameters of composites with different wall numbers, including transmission speed and temperature, according to the total entropy rate [6]. The results showed that, under the optimal parameters, the entropy rate and the friction volume of CNTs were significantly improved. Further, Guo, *et al*. described the impact of positive catalyst on Zinc–air battery [7]. In order to reduce production cost and improve the application value, bimetallic sulfide was proposed. By combining the vulcanization process with CNTs, it avoided the interference of S2 particles and accelerated the catalytic process. The results showed that the air battery under this method could maintain a long-term stable charging and discharging state.

Selective laser melting (SLM) technology is a 3D printing technique that constructs a three-dimensional model of an object and utilizes its data to achieve rapid prototyping of solid objects [8, 9]. SLM technology breaks free from the constraints of multiple processes and tools in traditional manufacturing processes, simplifies the processing process, and can maintain the accuracy and density of formed parts while ensuring the forming speed of large and complex shapes [10, 11]. Cheng, *et al*. explained the problem of low peak to average power in offset orthogonal amplitude modulation systems, analyzed the advantages and disadvantages of existing technologies, and proposed a cleared tissue digital scanned light-sheet microscopy (C-DSLM) method to address the shortcomings of the original method being too complex and difficult to implement [12]. It was proved that this method significantly reduced the complexity of operations and improved operational efficiency. Zong, *et al*. investigated the effect of laser inclination angle on the mechanical properties of Hastelloy x alloy [13]. The temperature changes during the alloy preparation process were analyzed by using finite element analysis method, and it was found that the inclination angle was positively correlated with the cooling rate. The results showed that, when the inclination angle was 30°, the tensile strength of the alloy reached 881.38 MPa with the best mechanical properties. Wei, *et al*. also studied the effect of laser energy input on the SLM forming of Ti-5Al-2.5Sn alloy, and analyzed the effect of low, medium, and high levels of Ev on the density and microstructure of the alloy through experiments [14]. The results showed that, when the Ev level was high, the density of the alloy material was higher. There were fewer strong textures, while the quality of the sample was higher. Due to the wide applicability of SLM technology to different materials, it plays an important role in the field of metal composite material forming. Among them, cast aluminum alloy is an aluminum alloy that obtains original parts through casting. SLM technology has a wide range of applications in manufacturing parts in aviation and automotive industries. While it has advantages such as low density, strong fluidity, and good corrosion resistance, it also has limitations such as poor wear resistance and low strength and hardness. Meanwhile, CNTs play an important role in the production of composite materials due to their performance advantages.

In order to optimize the forming technology of aluminum matrix composites, this study proposed the use of CNTs as reinforcing phases to prepare aluminum matrix composites by combined CNTs with SLM forming of aluminum matrix composites to improve the performance of aluminum matrix composites and the manufacturing level of aluminum matrix composites, which was innovative in improving the poor fatigue and low elastic modulus of cast aluminum alloy metals, reducing production costs, and promoting the development of the aluminum matrix composite material industry.

Materials and methods

Preparation of CNTs/Al composite powder

CNTs obtained from Chinese Academy of Sciences Chengdu Advanced Organic Chemistry Co., Ltd, Chengdu, Sichuan, China in different concentrations of 0.5, 1.0, 1.5, and 2.0 wt% were mixed with N-methylpyrrolidone (NMP) (Sinopharm Chemical Reagent, Shijiazhuang, Hebei, China) in the ratio of 1 g:100 mL, respectively, and placed in an ultrasonic shaker for 35 minutes to obtain the dispersion. Al powder was added to the mixture and stirred for 40 mins before drying in VOS-60A vacuum drying oven (Shidukai Instrument Equipment, Shanghai, China) to obtain the dispersion powder. A QM-SP2 type mechanical ball mill was applied to ground the powder at the rotational speed of 250 rpm for 12 hours to obtain the composite powders with different CNTs concentrations. The crystal plane spacing during the grinding process was calculated as follows:

$$d = \frac{a}{\sqrt{h^2 + k^2 + l^2}} \quad (1)$$

where *a* was the lattice constant. h, k, and l were the crystal plane indexes with the change of grinding time. The X-ray diffraction (XRD) phase analysis of CNTs and Al powders was performed to reduce the experimental errors. When the grinding time became shorter, the peak position of the derivative peak of the powder would move toward the large angle. The relationship between the crystalline surface spacing *d* and the derivative angle *Θ* was expressed in Equation (2).

$$n\lambda = 2d\sin\theta \quad (2)$$

where λ was the wavelength of the X-ray. *n* was the order of diffraction.

Finite element model for SLM forming of CNTs/Al composites

The prepared powders were subjected to SLM forming operation. A SLM forming finite element model was constructed, which included selecting the element type, dividing the mesh, and determining the thermal physical parameters. Solid85 was selected as the element of the finite element model, while the mapping method was selected to map the physical domain of the part to obtain the regular parameter domain. The grid was divided and mapped into Euclidean space to form an actual grid. It was assumed that CNTs/Al composite powders were isotropic, and their properties did not change with the change of direction. The initial condition of temperature distribution was calculated as

$$T_0(i, j, x) = T(i, j, x, t)|_{t=0} \quad (3)$$

where *T* was the temperature. *t* was the laser scanning time. T_0 was the initial temperature condition. *i*, *j*, and *x* were the length, width, and height of the grid, respectively. To ensure the existence of a deterministic solution to the control equation, it was necessary to determine the boundary conditions, including the variation laws of the four variables of temperature, heat flow density, medium temperature, and radiation heat dissipation during the SLM forming process. The temperature of the thermal conductor at the boundary at any time was calculated as

$$T(i, j, x)|_{t=s} = T \mid s(i, j, x, t) \quad (4)$$

where *s* was the boundary surface. The heat flow density on the object boundary was then calculated as

$$ke\frac{\partial T}{\partial y} = qs(i, j, x) \quad (5)$$

where *ke* was the effective thermal conductivity of the composite powder. *y* was the cosine of the boundary normal direction. *qs* was the gradient of the temperature. ∂ was the variation of the temperature as a function of the forward direction. The temperature of the fluid around the boundary surface and its surface heat transfer coefficient λ at any given moment were calculated as

$$ke\frac{\partial T}{\partial y} = \lambda(T_s - T_f) \quad (6)$$

where T_s was the temperature of the model surface. T_f was the temperature of the medium. The object underwent radiation heat transfer during the forming process, and the effective emissivity of the object was ε . Then the radiation heat dissipation operation at the boundary surface of the object was calculated as

$$ke\frac{\partial T}{\partial y} = \beta\varepsilon(T^4 - T_{env}^4) \quad (7)$$

where *β* was the Stephan-Boltzmann constant. T_{env} was the ambient temperature. The main heat exchange modes in the SLM forming process were heat radiation and heat convection. Then, the heat exchange boundary conditions of the model were shown as

$$-ke\frac{\partial T}{\partial y} = \alpha(T_s - T_0) \quad (8)$$

where *α* was the heat transfer coefficient. Based on the four boundary conditions and the specific heat capacity *c*, the controlling equation of temperature in SLM forming process could be derived as

$$pc\frac{\partial T}{\partial t} = ke(\frac{\partial^2 T}{\partial i^2} + \frac{\partial^2 T}{\partial j^2} + \frac{\partial^2 T}{\partial x^2}) + Q \quad (9)$$

where Q was the heat generated per unit volume. In this study, aluminum alloy was selected as the material of the substrate. When the temperature changed, the thermal physical parameters of the forming material and the substrate were basically the same and could be calculated as

$$Kp = K_b\frac{rm}{\pi}x \quad (10)$$

where K_b was the thermal conductivity of the aluminum alloy. *M* was the number of masses directly associated with the crystal. *r* was the relative density of the powder bed. *x* was the physical magnitude of the powder after being compressed. Briefly, CNTs/Al composite powder was placed inside the chamber of the SP101 SLM machine (Beifeng Intelligent Technology Co., Ltd., Suzhou, Jiangsu, China) and the composite powder was uniformly spread flat on the substrate by using a coating blade. A CAD 3D model was constructed by using the data of the part, and the 3D model was converted into a 2D cross-sectional pattern by the slicing and layering operation of Voxeldance Additive software (Mange Technology Co., Ltd., Shanghai, China) With a scan spacing of 85 μm, laser absorption of 40%, powder spreading time of 6 s, powder thickness of 22 μm, dot spacing of 80 μm, laser power of 340 W, and temperature control in the range of 2,500-2,900°C, the laser beam selectively melted the composite powder under the control of the scanning oscillator. After solidification, a solid consistent with the two-dimensional cross-sectional pattern was obtained. After obtaining the corresponding solids of each layer thickness, the final 3D sample was obtained by stacking layers together. Four kinds of aluminum matrix composites with different CNTs concentrations were obtained, and the aluminum alloy with zero CNTs was used as the experimental control. In addition, the aluminum alloy materials and aluminum matrix

composites with CNTs concentrations of 0 wt% and 1.5 wt% were employed to analyze the properties of sample materials including mechanical properties, thermal stability, and electrical conductivity under different SLM forming laser powers of 250 W, 280 W, 310 W, 340 W, and 370 W.

Inspection of CNTs/Al composites SLM forming

After SLM forming, the compactness, hardness, and wearability of CNTs/Al composites were inspected as the inspection indicators. The compactness was measured by using the Archimedes principle to measure the mass of samples in air (m_1) and water (m_2) by using HTPG312 electronic balance (Huachao Electric Appliances Co., Ltd, Wenzhou, Zhejiang, China) The calculation of the actual density P of samples was as follows.

$$p = \frac{m_1}{m_1 - m_2}(p_2 - p_1) + p_1 \tag{11}$$

where P_1 was the density of air and P_2 was the density of water. Then, the theoretical density P_3 could be derived as

$$p_3 = \frac{p_a \times p_b}{p_a m_a + p_b m_b} \tag{12}$$

where P_a was the density of the aluminum matrix and P_b was the density of CNTs. m_a was the mass of the aluminum matrix and m_b was the mass of the CNTs. The hardness reflects the loading capacity of the composite material to the pressure of a hard object and is one of the mechanical properties characterized by the operation of the theoretical hardness H. The hardness was tested by using HV G50 micro dimensional hardness tester (Daming Optical Instrument Co., Ltd, Beijing, China) and was calculated as follows.

$$H = H_a V_a + H_b V_b \tag{13}$$

where H_a and H_b were the hardness of the aluminum matrix and CNTs, respectively. V_a and V_b were the volume of the aluminum matrix and CNTs, respectively. The wearability is the loss of composite materials due to friction and is usually expressed as a change in material mass and volume, and was measured by using Tecnai 20 transmission electron microscope (FEI Company, Hillsboro, Oregon, USA). The wearing volume V was calculated as

$$V = \frac{M}{p} \tag{14}$$

where M was the mass of the sample lost after friction. The wearing rate of the sample could be determined by the wearing volume ϖ , which was calculated as

$$\varpi = \frac{V}{PL} \tag{15}$$

where P was the base joint error and tooth shape error generated during the wearing process. L was the translation distance between the crystal surfaces.

The conductivity of CNTs/Al composites was investigated by using JEM-2100 transmission electron microscopy (TEM) (JEOL, Peabody, MA, USA) with the acceleration voltage of 200 kV to study the morphology of initial surface microhardness (ISMH) and surface microhardness (SMH), as well as the dispersion of filler in the composite. Briefly, a diluted CNTs/Al composites dispersed droplet was placed on a copper grid, covered with filter paper, and dried under a fluorescent lamp before EMFC7 ultra-thin slicer (Leica Microsystems GmbH, Wetzlar, Germany) was used to obtain adhesive samples for observation. In addition, the microstructures and morphologies of different sample materials were inspected and compared by using optical and scanning electron microscopy while the densities, hardness, and wearing coefficients were used as performance test indexes to analyze the effects of CNTs concentration on the properties of aluminum matrix composites.

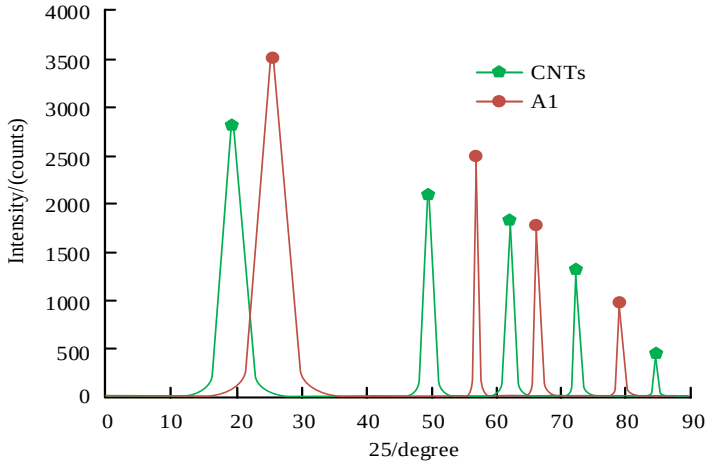

Figure 1. XRD patterns of CNTs and Al powders.

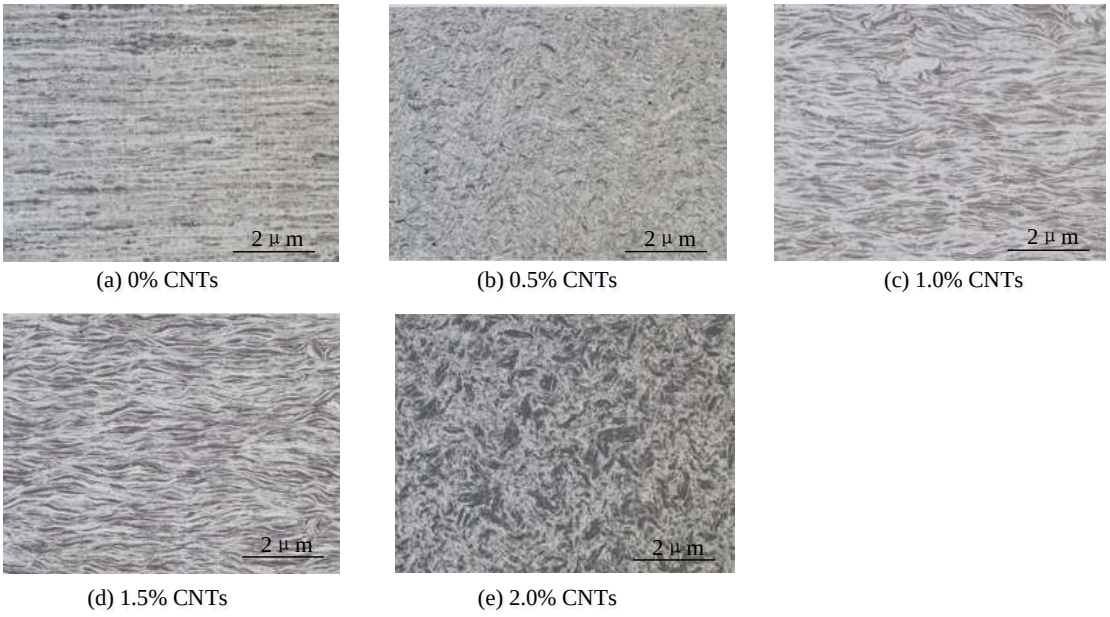

Figure 2. Comparison of microstructure and morphology of specimen materials.

Results and discussion

Properties of aluminum matrix composites with different CNTs concentrations

The XRD patterns of CNTs and Al powders were shown in Figure 1. The diffraction peaks of CNTs and Al powders were compared by using the eight strong peak matching standard PDF cards. The results showed that the diffraction peaks of carbon and Al represented for CNTs and Al powders, respectively, demonstrated no impurity peaks of other elements, which indicated the high purities of both CNTs and Al powders. The constituent unit of CNTs is carbon atoms, which form graphite sheets based on the hexagonal structure formed by the interconnection between carbon atoms. The graphite sheets bend around the central axis to form the CNTs structure. Due to this special structure, CNTs have a great aspect ratio, extremely high softness, and the advantages of graphite heat resistance and heat transfer.

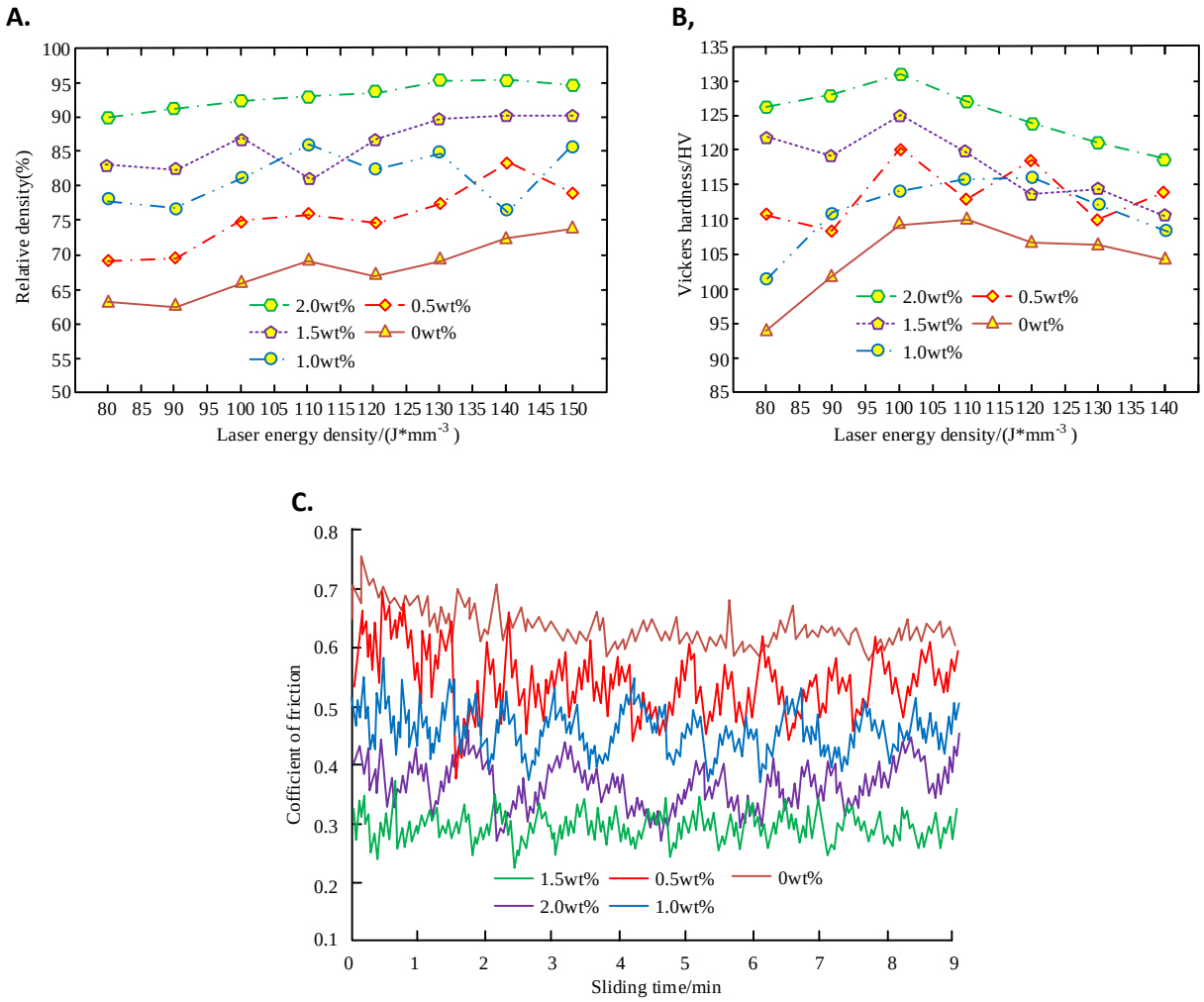

Figure 3. Density (**A**), hardness (**B**), and wearing coefficient (**C**) of forming materials with different CNTs concentrations.

Therefore, CNTs are often used to enhance composite materials [15]. The combination of CNTs and Al alloy materials was beneficial for improving the low mechanical properties of aluminum matrix composites and enhancing their application value. Through the observation of the microstructure and morphology of the sample material, the results showed that, with the increase of CNTs concentration, the internal structure of the sample material was clearly layered with more details being observed (Figure 2), while the grains tended to epitaxial along the formation direction (Figure 2b to 2e). The cross-section observation found that the cell crystals were uniformly distributed, and the crystal grains were very small (Figure 2e). During the forming process, when the liquid phase in the molten pool solidified rapidly, CNTs and Al powder precipitated grains together. Due to different solidification times, the grains exhibited a trend of epitaxial growth. Meanwhile, factors such as lava flow and high temperature during the formation process accelerated the reflection of the original materials at the interface, which was beneficial for improving the strength of the specimen material. The density of the aluminum matrix composite material was at the highest level of 90-95% with the minimum change when CNTs concentration was 2 wt% (Figure 3A). The density increased steadily with the increase of laser energy. The density of the composite material with 1.5 wt% CNTs remained stable in

the range of 80-88%. The highest density of the material reached 85% when CNTs concentration was 1 wt%, while the minimum density of 76% was observed at the same CNTs concentration. The aluminum alloy material with the lowest overall density was the one that had no CNTs with the density range of 63-70%. Overall, adding CNTs to the SLM forming of aluminum matrix composites could greatly improve the density of the composite material, reduce pores and gaps, and enhance the stability of the crystal structure. The hardness of the formed material under different CNTs contents was shown in Figure 3B. The aluminum matrix composite material with the best hardness performance was the one with 2 wt% CNTs. When the laser energy was 100 J/mm^3, the hardness reached the highest of 130 HV, while, when the laser energy was 140 J/mm^3, the hardness reached the lowest level of 120 HV. When the CNTs concentration was 1.5 wt%, the hardness of the composite material varies within the range of 112-122 HV. Among several formed samples, the aluminum alloy material had the lowest hardness effect, with the highest and lowest hardness being 94 HV and 110 HV, respectively. Compared to the aluminum matrix composite material with 2 wt% CNTs, the hardness decreased by 26 HV and 20 HV, respectively. Overall, increasing the concentration of CNTs was beneficial for improving the hardness of aluminum matrix composites and enhancing their resistance to pressure. The wearing coefficient of formed materials in different CNTs concentrations was shown in Figure 3C. The aluminum matrix composite material with 1.5 wt% CNTs showed the lowest wearing coefficient of 0.3 without significant fluctuations, while the composite material with 0.5 wt% CNTs demonstrated the largest change in wearing coefficient with the lowest and highest wearing coefficients reaching 0.38 and 0.7, respectively. The composite materials with 1 wt% and 2 wt% CNTs had good wearing resistance with their wearing coefficients maintained within the ranges of 0.38 - 0.53 and 0.28 - 0.43, respectively. The wearing coefficient of aluminum alloy material was stable at around 0.65, which was about 0.35 higher than that of the composite material with the best wear resistance. Overall, adding a certain amount of CNTs could significantly optimize the friction performance of aluminum matrix composites, reduce the wearing rate of the composite, and effectively enhance the resistance of the composite to mechanical wearing. Adding different concentration of CNTs could effectively improve conductivity (Figure 4). Through the comparison of three different CNTs concentrations in the aluminum-based loading materials, the conductivities of 2.0 wt% CNTs was the fastest one, while that of 1.0 wt% CNTs was relatively slow. Overall, increasing the concentration of CNTs helped to improve the conductivity of the material. The results showed that the maximum conductivities were increased by 1.51×10^5, 4.62×10^5, and 6.91×10^5 when 1.0 wt%, 1.5 wt%, and 2.0 wt% CNTs were added, respectively.

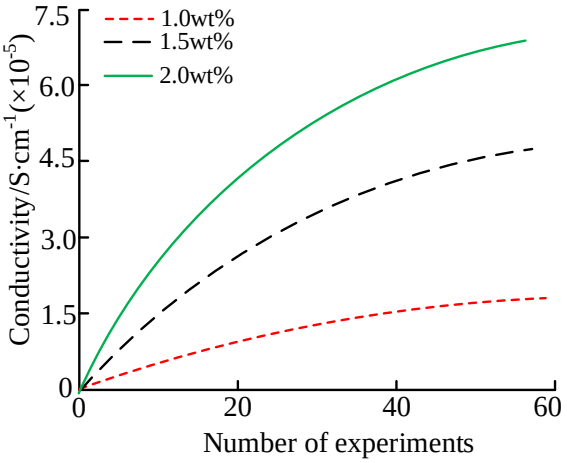

Figure 4. The effects of different CNTs concentrations on the conductivity of aluminum-based loading materials.

Aluminum matrix composite properties under different laser process parameters

The stress-strain curves of the formed materials at different laser powers were shown in Figure 5. The strength of the aluminum matrix composite material with 1.5 wt% CNTs reached the highest value of 410 MPa and the lowest values of 260 MPa at laser power of 370 W and 250 W, respectively, while its elongation was 8.7% and

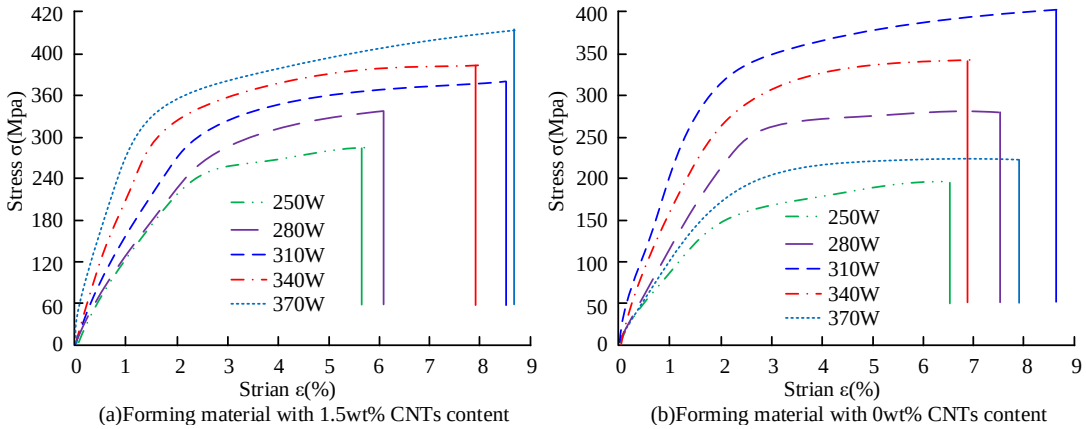

Figure 5. Stress strain curves of forming materials under different laser power.

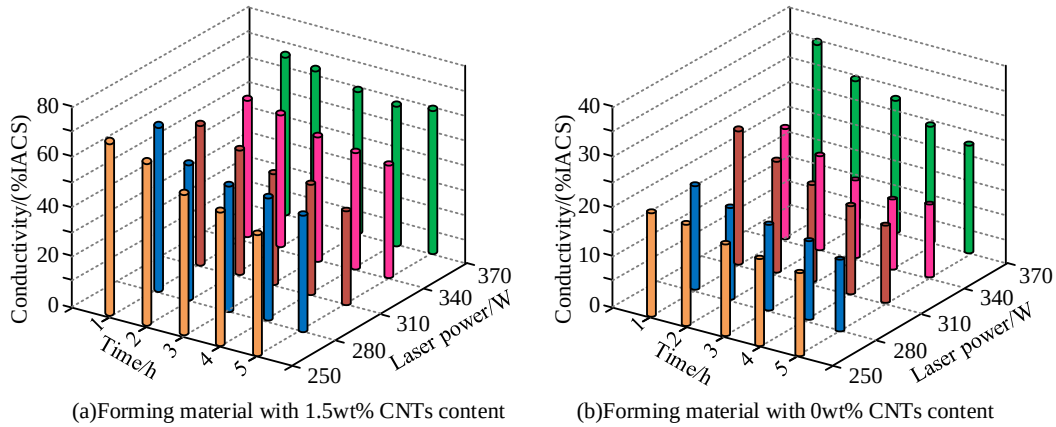

Figure 6. Conductivity of forming materials under different laser power.

5.8%, respectively. When the laser power was 310 W, the elongation of the composite material reached 8.5% and the strength and elongation of aluminum alloy materials were 360 MPa and 8.6%, respectively, indicating the best mechanical properties. On the other hand, the aluminum alloy material with 0 wt% CNTs formed under 250 W laser power demonstrated the lowest strength and elongation levels of 170 MPa and 6.6%, respectively. Overall, the strength and elongation of forming materials containing CNTs were higher than those of aluminum alloy materials, which suggested that adding CNTs to the Al matrix was beneficial for improving the load-bearing capacity of the formed material, enhancing its ductility, and optimizing the mechanical properties of the aluminum matrix composite material. The conductivity of the formed material under different laser powers was shown in Figure 6. The composite material with 1.5 wt% CNTs formed by SLM at a laser power of 370 W showed the highest conductivity within the range of 60-68% International Annealed Copper Standard (IACS), while the material formed with a laser power of 250 W had the best conductivity of 60% IACS at 1 hour. The material with the worst conductivity was formed under 310 W laser power with the conductivity ranged from 48 to 52% IACS (Figure 6a). On the other hand, the material with 0 wt% CNTs demonstrated the worst conductivity at 280 W laser power with the highest and lowest conductivity of 18% IACS and 15% IACS, respectively. Compared to the same material

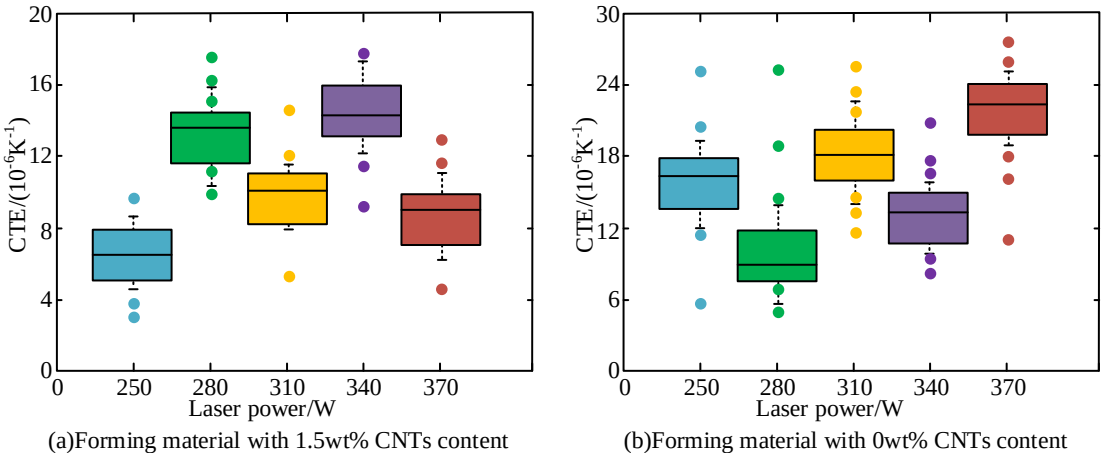

Figure 7. Coefficient of thermal expansion (CTE) of forming material under different laser power.

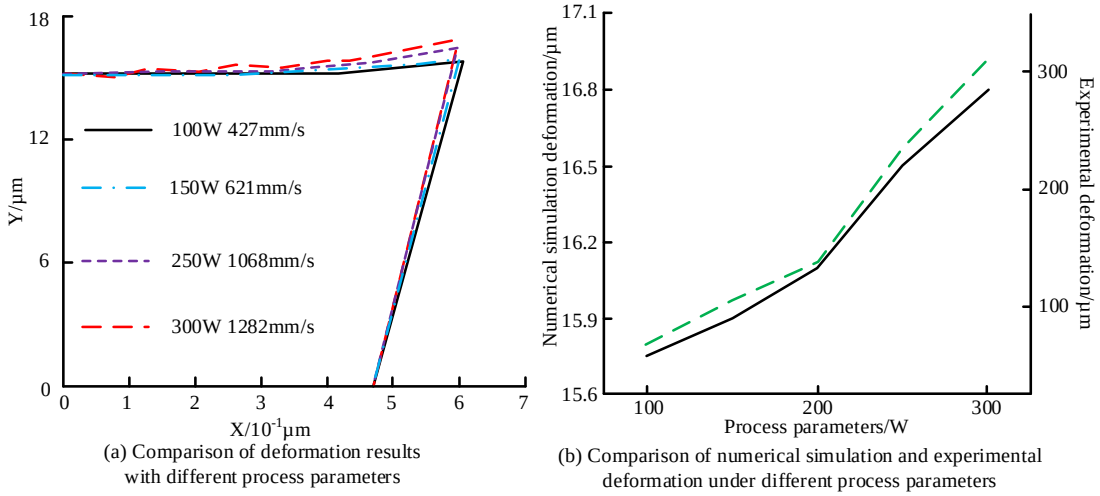

Figure 8. Actual results of finite element model analysis using SLM forming.

formed at 370 W power, the highest and lowest conductivity were reduced by 17% IACS and 5% IACS, respectively (Figure 6b). Overall, adding CNTs to aluminum matrix composites could effectively improve the limitation of low conductivity of aluminum alloy materials and enhance the application value of composite materials. The coefficient of thermal expansion of the formed material under different laser power was shown in Figure 7. The coefficient of thermal expansion (CTE) of the material formed by adding 1.5 wt% CNTs reached the highest level of 14×10^{-6}/K and the lowest level of 7×10^{-6}/K for the laser powers of 340 W and 250 W, respectively. The overall CTE was low. The CTE of the formed materials kept at the lower levels of 9×10^{-6}/K and 10×10^{-6}/K for the laser power of 370 W and 310 W, respectively (Figure 7a). However, the CTE of the SLM formed material without CNTs was 24×10^{-6}/K at the highest and 8×10^{-6}/K at the lowest, corresponding to laser powers of 370 W and 280 W, respectively. The CTE was increased by 10×10^{-6}/K and 1×10^{-6}/K, respectively, compared to that of the aluminum matrix composite with 1.5 wt% CNTs (Figure 7b). Overall, adding CNTs could reduce the impact of temperature on composite materials and enhance their stability at high temperatures. The

results of this study indicated that adding CNTs to laser selective melting forming of aluminum matrix composites could effectively optimize the mechanical properties of aluminum matrix composites and improve their conductivity, thermal stability, and other properties.

The deformation of CNTs/Al composites

The deformation of CNTs under different process parameters was analyzed by using the SLM forming finite element model and the comparison between numerical simulation and experimental deformation of the model. The results showed that the temperature field distribution of SLM formed parts was better when the laser power was 100 W and scanning speed was 427 mm/s. There was good similarity between numerical simulation deformation and experimental deformation under the different process parameters, and the simulation model showed good reliability under different process parameters (Figure 8). Overall, the finite element model constructed in this study had well analyzed the changes in SLM forming with high effectiveness.

Conclusion

Cast aluminum alloy is an important casting material with extensive applications in fields such as coal mining and excavation, ship shipping, and aviation industry. In order to optimize the laser selective melting technology of aluminum matrix composites, a SLM forming method based on CNTs for aluminum matrix composites was proposed in this study. The performance of the composite materials was tested and analyzed. The results showed that, when the content of CNTs was 2 wt%, the density and hardness of aluminum based composite materials were the highest with the increase of 20-27% and 20 HV compared to that of aluminum alloy materials. When the content of CNTs was 1.5 wt%, the wearing coefficient of aluminum matrix composite material was the lowest and stable at around 0.3 compared to that of aluminum alloy material at 0.65. When the laser power was 370 W, the strength and elongation of aluminum based composite materials were the highest at 410 MPa and 8.7%, respectively, while the conductivity reached the high-level ranged from 60-68% IACS. The maximum CTE of aluminum matrix composites was 14×10^{-6}/K, which was reduced by 10% compared to aluminum alloy materials. The SLM forming finite element model constructed in this study had high practical application effectiveness. The results suggested that CNTs could improve the uniformity of microstructure in aluminum matrix composites, reduce pores, increase density, enhance the stability of aluminum matrix composites under pressure, wearing, and high temperatures simultaneously, improve the performance, and meet the needs of industrial production.

Acknowledgement

This research was supported by Natural Science Research Project of Higher Education Institutions in Anhui Province, China (Grant No. KJ2021A1309).

References

1. Shen M, Gao K, Duan C, Hu W, Ding S, Yang G, *et al*. 2021. Coordination-driven hierarchically structured composites with N-CNTs-grafted graphene-confined ultra-small Co nanoparticles as effective oxygen electrocatalyst in rechargeable Zn-air battery. Ceram Int. 47(21):30091-30098.
2. Peng J, He Y, Zhou C, Su S, Lai BL. 2021. The carbon nanotubes-based materials and their applications for organic pollutant removal: A critical review. Chinese Chem Lett. 32(5):1626-1636.
3. Xue W, Yang G, Bi S, Zhang J, Hou ZL. 2021. Construction of caterpillar-like hierarchically structured Co/MnO/CNTs derived from MnO_2/ZIF-8@ZIF-67 for electromagnetic wave absorption. Carbon. 173(48):521-527.
4. Bairagi S, Ali W. 2020. Investigating the role of carbon nanotubes (CNTs) in piezoelectric performance of PVDF/KNN based flexible electrospun nanogenerator. Soft Matter. 16(20):4876-4886.
5. Wang Z, Sun X, Min B. 2021. Development of novel TPI/HDPE/CNTs ternary hybrid shape memory nanocomposites. Nanotechnology. 32:405706.
6. Khan SA, Saeed T, Khan MI, Hayat T, Khan M I, Alsaedi A. 2019. Entropy optimized CNTs based darcy-forchheimer nanomaterial flow between two stretchable rotating disks. Int J Hydrogen Energ. 44(59):31579-31592.

7. Guo J, Xu N, Wang Y, Wang X, Huang H, Qiao J. 2020. Bimetallic sulfide with controllable Mg substitution anchored on CNTs as hierarchical bifunctional catalyst toward oxygen catalytic reactions for rechargeable Zinc-Air batteries. ACS Appl Mater Interfaces. 12(23):37164-37172.
8. Geenen K, Röttger A, Feld F, Theisen W. 2019. Microstructure, mechanical, and tribological properties of M3:2 high speed steel processed by selective laser melting, hot- isostatic pressing, and casting. Addit Manuf. 28:585-599.
9. Ferreira AF, Chrisóstimo WB, Sales RC, Garção, WJL, de Paula Sousa N. 2019. Effect of pouring temperature on microstructure and microsegregation of as-cast aluminum alloy. Int J Adv Manuf Tech. 104(1):957-965.
10. Wang P, Eckert J, Prashanth KG, Wu MW, Kaban I, Xi LX, *et al*. 2020. A review of particulate-reinforced aluminum matrix composites fabricated by selective laser melting. T Nonferr Metal Soc. 30(8):2001-2034.
11. Otani Y, Kusaki Y, Itagaki K, Sasaki S. 2019. Microstructure and mechanical properties of A7075 alloy with additional Si objects fabricated by selective laser melting. Mater Trans. 60(10):2143-2150.
12. Cheng X, Liu D, Shi W, Zhao Y, Li Y, Kong D. 2020. A novel conversion vector-based low-complexity SLM scheme for PAPR reduction in FBMC/OQAM systems. IEEE T Broadcast. 66(3):656-666.
13. Zong X, Zhang J, Fu H. 2021. Effect of laser inclination angle on mechanical properties of hastelloy x processed by selective laser melting. Mater Test. 63(1):10-16.
14. Wei K, Zeng X, Huang G, Deng J, Liu M. 2019. Selective laser melting of Ti-5Al-2.5Sn alloy with isotropic tensile properties: The combined effect of densification state, microstructural morphology, and crystallographic orientation characteristics. J Mater Process Tech. 271:368-376.
15. Moeini G, Sajadifar SV, Wegener T, Rößler, C, Gerber A, Böhm S, *et al*. 2021. On the influence of build orientation on properties of friction stir welded Al-Si10Mg parts produced by selective laser melting. J Mater Res Technol. 12:1446-1460.